Option Valuation under Stochastic Volatility

With Mathematica Code

Published by: Finance Press, Newport Beach, California, USA
Cover design by: Brian Burton Design

For the latest available updates and corrections to this book and publisher contact information, visit the Internet sites:
http:// www.financepress.com or http://members.home.net/financepress

International Standard Book Number 0-9676372-0-1
Library of Congress Card Number: 99-91935

Printed in the United States of America
Printed on acid-free paper

6 The Term Structure of Implied Volatility

The term structure of implied volatility is the relation between the option implied volatility and time to maturity: $\sigma^{imp}(\tau)$. Using our previous notation, it's the square root of $V^{imp}(X,V,\tau)$, holding the moneyness X and the initial volatility V fixed. In practice, the implied volatility is usually measured at a strike price close to the money. ($X=0$ is a natural choice). In fact, the qualitative behavior is the same at any strike: a graph of $\sigma^{imp}(\tau)$ vs. τ ultimately flattens to a limiting asymptotic value, $\sigma_{\infty}^{imp}=(V_{\infty}^{imp})^{1/2}$, that is independent of both X and V. This general behavior is analogous to the term structure of interest rates and the existence of a long-run rate of interest.

The asymptotic implied volatility depends only upon the parameters of the volatility process. It can be calculated from the simple relation

$$V_{\infty}^{imp}=8\lambda(k_0)\,,$$

where λ is the first eigenvalue of a differential operator, and k_0 is a complex number. We illustrate 3 ways to calculate V_{∞}^{imp} for general models: a series method, a variational method, and a differential equation-based method. Computation times for the latter two methods are just a couple of seconds in Mathematica.

1 Deterministic Volatility

The volatility models that we consider in this book typically have a similar structure: $dV_t = b(V_t)dt + a(V_t)dW_t$, where the drift term $b(V_t)$ exhibits mean-reversion. For example, the GARCH diffusions and other models have the linear drift form $b(V_t) = \omega - \theta V_t$, where ω and θ are positive constants. If the volatility becomes small, then $b(V_t)$ is positive, causing the volatility to tend to grow larger. If the volatility is large, then $b(V_t)$ is negative, causing the volatility to tend to grow smaller.

To a first approximation, the term structure is explained by letting the Brownian noise term vanish[1]. For the linear drift models, we are left with the deterministic volatility evolution $\dot{V}_t = \omega - \theta V_t$, where the dot means a time derivative. The solution to the differential equation $\dot{y} = \omega - \theta y$, where $y(0) = V$ is given by

$$y(t,V) = \frac{\omega}{\theta} + (V - \frac{\omega}{\theta})e^{-\theta t}. \tag{6.1}$$

In (6.1), the behavior is especially simple as $t \to \infty$; no matter what the starting value V, the volatility tends to the fixed point $V^* = \omega / \theta$. This value is called a fixed point because if the volatility starts there, it stays there. The fixed point is *attractive* or *stable* because small departures of the volatility from V^* are damped over time.

Option valuation under deterministic volatility is a well-known application of the B-S theory. Options are still priced by the B-S formula, but the volatility parameter in the formula is modified. The modified volatility is simply the time-average of the deterministic volatility. In other words, if $C(S,V,\tau)$ is the general call option value and $c(S,V,\tau)$ is the B-S value, then under deterministic volatility:

[1] For simplicity, we call the term structure of implied volatility just the term structure. With the exception of one subsection, in this chapter the risk-adjusted volatility process and the actual volatility process are assumed identical (a risk-neutral world). See Chapter 8 (Duality and Changes of Numeraire) to convert the results in this chapter to log-utility.

(6.2) $$C(S,V,\tau) = c\left(S,\mu(V,\tau),\tau\right),$$

where $$\mu(\tau,V) = \frac{1}{\tau}\int_0^\tau y(s,V)\,ds = \frac{\omega}{\theta} + \left(V - \frac{\omega}{\theta}\right)\left(\frac{1-e^{-\theta\tau}}{\theta\tau}\right).$$

The B-S implied volatility is given by $\sigma^{imp}(\tau,V)] = [\mu(\tau,V)]^{1/2}$.

Shown in Fig. 6.1 is a plot of both $\sigma^{imp}(\tau,V)$ and $[y(\tau,V)]^{1/2}$ versus τ, where $\omega_a = 0.02$ and $\theta_a = 2$, (annualized parameters). We show two cases: (i) initial volatility $\sigma_a = 8\%$ $(V_a = 0.0064)$ and (ii) initial volatility $\sigma_a = 12\%$ $(V_a = 0.0144)$. Notice that the implied volatility (the bold line) behaves a lot like the actual volatility $y(\tau,V)$ (the thin line); the only difference is that the implied volatility changes more slowly because it's a time-average. But both functions begin at V and evolve in a smooth monotonic fashion with a limiting asymptotic value $\sigma_\infty^{imp} = (\omega/\theta)^{1/2} = 10\%$. The asymptotic value is independent of the starting value V, as well as S, K, r, and δ.

The rate of convergence to the asymptotic value is determined by the parameter θ, which has the dimensions $[1/\tau]$. Since the "decay rate" is determined by the exponential term $\exp(-\theta\tau)$, this type of behavior is often described as having a "half-life" $\tau_{1/2} = 1/\theta$. In our example, $\tau_{1/2} = 0.5$ years and one can see from Fig 6.1 that both the actual and implied volatilities have moved, very roughly, about half-way toward their final asymptotic value at $\tau = 0.5$ years.

Many other models of interest to researchers have a deterministic limit that behaves in the same way as this example. In general, volatility evolution in the deterministic limit is $\dot{V}_t = b(V_t)$, where $b(\cdot)$ is the drift coefficient. If a model is mean-reverting, $b(V)$ will typically have a single zero at some $V = V^*$. The zero will be attractive, meaning not only $b(V^*) = 0$ but also $b'(V^*) < 0$, where the prime means a derivative. If you picture the graph of $b(V_t)$ you can see that the volatility evolution will be similar to Fig. 6.1. It follows from $\dot{V}_t = b(V_t)$ that $b(V)$ has the dimensions of $[V/t]$, so that $b'(V^*)$ has the dimensions $[1/t]$. This causes $|1/b'(V^*)|$ to play the role of the half-life parameter in general models, at least asymptotically.

Fig. 6.1 Term Structure of Implied Volatility (Deterministic Model)

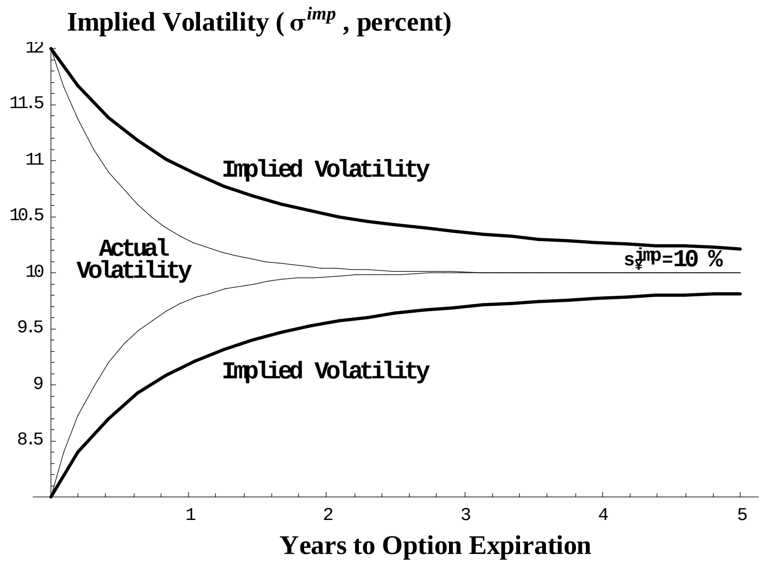

Fig. 6.2 Term Structure of Implied Volatility (Stochastic Model)

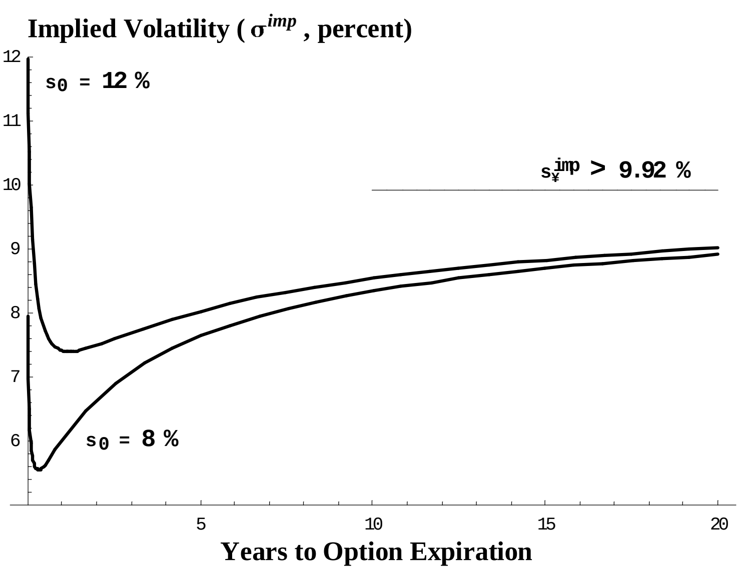

2 Deterministic Volatility II: a Transform Perspective

In the last section we showed that the deterministic volatility model $\dot{V}_t = \omega - \theta V_t$ has an asymptotic implied volatility $V_\infty^{imp} = \omega / \theta$. In this section we consider this same problem with the transform method. The advantage of the transform method is that it also solves the case we are really interested in—stochastic volatility.

Call option Solution II of (**2**.2.10) is:

$$(2.1) \quad C(S,V,\tau) = Se^{-\delta\tau} - Ke^{-r\tau} \frac{1}{2\pi} \int_{ik_i-\infty}^{ik_i+\infty} e^{-ikX} \frac{\hat{H}(k,V,\tau)}{k^2 - ik} dk\,, \quad 0 < \operatorname{Im} k < 1\,.$$

The natural strike price K at which to measure the term structure is given by $X = 0$, which corresponds to $Ke^{-r\tau} = Se^{-\delta\tau}$. If $r \neq \delta$ and you measure at $K = S$, you are systematically moving to one side of the volatility smile pattern as the time to expiration increases. With the better choice $X = 0$, (2.1) simplifies to:

$$(2.2) \qquad \frac{C(S,V,\tau)}{Ke^{-r\tau}} = 1 - \frac{1}{2\pi} \int_{ik_i-\infty}^{ik_i+\infty} \frac{\hat{H}(k,V,\tau)}{k^2 - ik} dk$$

We established in Chapter 2 that, under constant volatility, this solution was valid for the entire strip $0 < \operatorname{Im} k < 1$. The same holds true under deterministic volatility because, as we will show, $\hat{H}(k,V,\tau)$ is an entire function under either constant or deterministic volatility.

We established the solution for the fundamental transform $\hat{H}(k,V,\tau)$ under deterministic volatility in Appendix 3.1 at (**3**.A.2). For the drift function $b(V) = \omega - \theta V$, that formula becomes

$$\hat{H}^{(0)}(k,V,\tau) = \exp[-c(k)U(V,\tau)]\,, \quad \text{where } c(k) = \tfrac{1}{2}(k^2 - ik)\,,$$

and
$$U(V,\tau) = \int_0^\tau y(s,V)\,ds = \frac{\omega}{\theta}\tau + \left(V - \frac{\omega}{\theta}\right)\left(\frac{1 - e^{-\theta\tau}}{\theta}\right).$$

This shows that $\hat{H}^{(0)}(k)$ is an entire function of k in the complex k-plane. A general plot of the modulus $|\hat{H}^{(0)}(k)|$ has already been given in Chapter 2, Fig. 2.1. The asymptotic theory considers $\tau \to \infty$. Suppose we are integrating in (2.1) along $\operatorname{Im} k = 1/2$. In Fig. 6.3, we plot $|\hat{H}^{(0)}(k_r + i/2)|$ versus k_r for

$\tau = 5$, 20, and 100 years, using the previous numerical example $\omega_a = 0.02$, $\theta_a = 2$, and $V_a = 0.0064$.

Fig. 6.3. $|\hat{H}(k)|$ along an Integration Contour (Im k = 1/2) Various Times to Maturity τ (Deterministic Model)

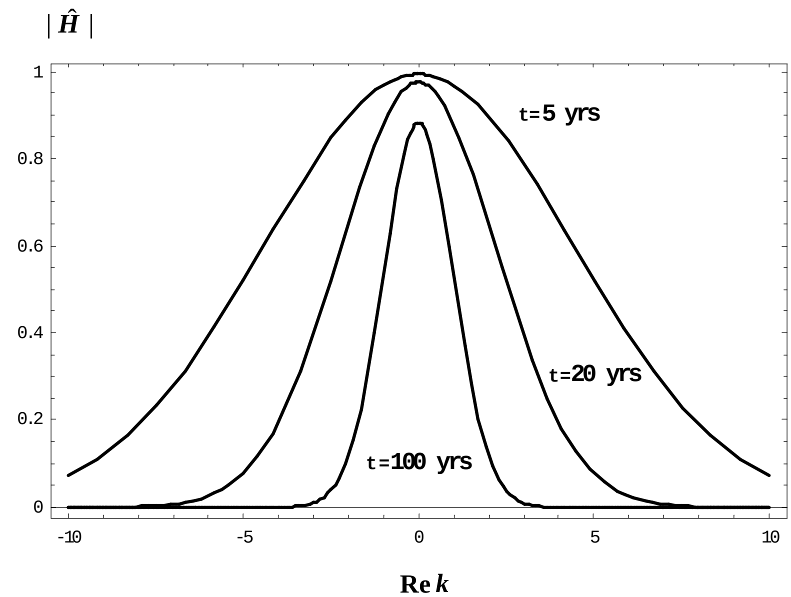

As you can see from Fig. 6.3, the fundamental transform becomes increasingly peaked about $k_r = 0$ as the time to maturity increases. For $\tau >> 1$, (2.2) becomes

$$\frac{C(S,V,\tau)}{Ke^{-r\tau}} \underset{\tau\to\infty}{\approx} 1 - \frac{1}{2\pi}\int_{ik_i-\infty}^{ik_i+\infty} \exp\left[-c(k)\frac{\omega}{\theta}\tau - c(k)\frac{1}{\theta}\left(V - \frac{\omega}{\theta}\right)\right]\frac{dk}{k^2 - ik}$$

Of course because this is the B-S theory, we could evaluate this integral exactly (see Chapter 2, Appendix 1). But an alternative method will also work in the stochastic volatility case: the asymptotic method of steepest descent.[2] As $\tau \to \infty$, Fig. 6.3 shows that the exponential factor in the integral damps the contribution everywhere except near $k_r = 0$, which is our integration origin. If

---

[2] For a nice discussion of the methods of steepest descent, saddle points, and the method of stationary phase, see Carrier, Krook, and Pearson (1966, Chapt. 6).

we didn't know this point, we could find it by looking for the stationary point k_0 determined by $c'(k_0) = 0$, which has the solution $k_0 = i/2$. This solution k_0 is also a *saddle point* because, while the modulus $|\hat{H}|$ is decreasing in the real direction, it's increasing in the imaginary direction (see Fig. 2.1 in Chapter 2). Along this integration contour, $c(k) = 1/8 + k_r^2/2$. This is an exact relation, but in the stochastic case (see below), we will expand the integrand in a Taylor series about the saddle point. In this special case, the Taylor series only has the two terms. The leading asymptotic contribution to the integral is given by

$$\frac{C(S,V,\tau)}{Ke^{-r\tau}} \underset{\tau\to\infty}{\approx} 1 - \frac{4}{2\pi}\exp\left(-\frac{\omega}{8\theta}\tau\right)\exp\left[-\frac{1}{8\theta}\left(V-\frac{\omega}{\theta}\right)\right]\int_{-\infty}^{\infty}\exp\left(-k_r^2\frac{\omega}{2\theta}\tau\right)dk_r$$

The integral that remains is just a Gaussian

$$\int_{-\infty}^{\infty}\exp\left(-k_r^2\frac{\omega}{2\theta}\tau\right)dk_r = \sqrt{\frac{2\pi\theta}{\omega\tau}}\,.$$

So we obtain the result

$$\frac{C(S,V,\tau)}{Ke^{-r\tau}} \underset{\tau\to\infty}{\approx} 1 - \sqrt{\frac{8\theta}{\pi\omega\tau}}\exp\left[-\frac{1}{8\theta}\left(V-\frac{\omega}{\theta}\right)\right]\exp\left(-\frac{\omega}{8\theta}\tau\right).$$

This result can be compared with the Black-Scholes formula, which is easily shown to be, in this limit,

$$\frac{c(S,V,\tau)}{Ke^{-r\tau}} \underset{\tau\to\infty}{\approx} 1 - \sqrt{\frac{8}{\pi V\tau}}\exp\left(-\frac{V}{8}\tau\right). \tag{2.3}$$

Comparing the last two equations implies that $V_\infty^{imp} = \omega/\theta$, just as we expected. The important idea is that we now have a method for the stochastic case.

3 Stochastic Volatility—The Eigenvalue Connection

Notice that as $\tau \to \infty$, the fundamental transform in the previous section had the following special form

$$\hat{H}^{(0)}(k,V,\tau) = \exp[-c(k)U(V,\tau)] \underset{\tau\to\infty}{\approx} \exp[-\lambda(k)\tau]\,u(k,V),$$

where

$$\lambda(k) = c(k)\frac{\omega}{\theta} \quad \text{and} \quad u(k,V) = \exp\left[-c(k)\frac{1}{\theta}\left(V-\frac{\omega}{\theta}\right)\right].$$

This form is special because, first of all, the dependence upon V and τ has *separated* into the product of two terms, one depending upon τ and one depending upon V. (Both terms depend upon k) . Suppose, that under stochastic volatility, the same form of solution holds:

$$\hat{H}(k,V,\tau) \underset{\tau\to\infty}{\approx} \exp[-\lambda(k)\tau]\, u(k,V) \tag{3.1}$$

with new functions $\lambda(k)$ and $u(k,V)$ to be determined. If we substitute this form into the PDE (**2**.2.19) satisfied by the fundamental transform, then we are left with the ordinary differential equation for $u(k,V)$:

$$\mathcal{L}_k\, u = \lambda(k)\, u\,, \tag{3.2}$$

where

$$\mathcal{L}_k u = -\tfrac{1}{2} a^2(V) \frac{d^2 u}{dV^2} - \left[\tilde{b}(V) - ik\rho(V)a(V)V^{1/2}\right]\frac{du}{dV} + c(k)V\, u\,.$$

This is an *eigenvalue* equation, where $\lambda(k)$ is an eigenvalue of the differential operator $\mathcal{L}_k$, and u is the associated *eigenfunction.*[3]. In general, there can be many solutions to (3.2). In fact, you may be able to develop the fundamental transform at all times τ (not just $\tau \to \infty$) as a sum over such solutions—this is called an *eigenfunction expansion*[4]. But, in the limit $\tau \to \infty$, the dominant term of such a sum uses the *smallest* or *first* eigenvalue. This may seem confusing at this point because there are a lot of complex numbers appearing in (3.2), so what do we mean by smallest? Below, we show that, in fact, everything we calculate is real-valued and the first or smallest eigenvalue is well-defined.

What does the first eigenfunction look like? In Fig. 6.4 we show plots of $u(k,V)$ vs. V with $k = i/2$. The model is the GARCH diffusion process $dV = (\omega - \theta V)\,dt + \xi V dW(t)$, with $\omega = 0.02$, $\theta = 2$, $\xi = 1.5$ and $\rho = -1, 0, 1$. How we calculated that function is explained in Sec. 8.

---

[3]Eigenvalue problems are not well-defined until we specify a class of admissible functions. This is discussed later in Sec. 7

[4] See my article (Lewis 1998).

Fig. 6.4 First Eigenfunction for the GARCH Diffusion Process

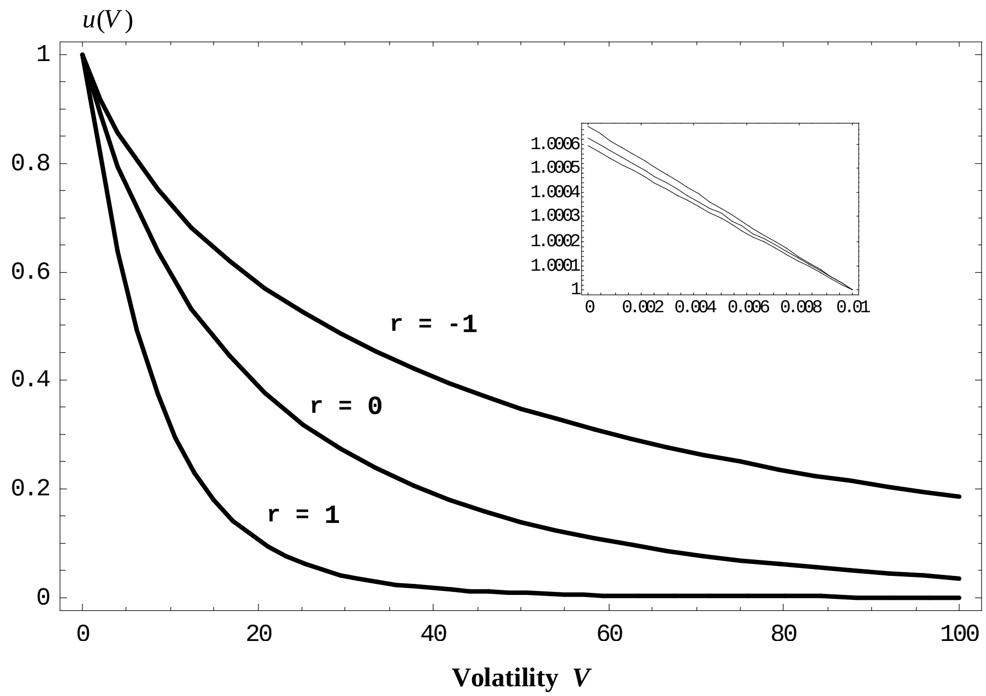

Notes. The figure shows a plot of the first eigenfunction $u(k,V)$ for the GARCH diffusion model, $dV = (\omega - \theta V)\,dt + \xi V dW(t)$, with $\omega = 0.02$, $\theta = 2$, $\xi = 1.5$ and $\rho = -1, 0, 1$. The parameter k is set to $i/2$ The function has been normalized so that $u(V = \omega/\theta) = 1$. Since $\omega/\theta = 0.01$, the range $V < \omega/\theta$ is difficult to resolve in the scale of the main plot and is shown in the inset. The Mathematica code for this plot is given in the Appendix to this chapter.

With this general form of solution, then (2.2) becomes in the stochastic case:

$$\frac{C(S,V,\tau)}{Ke^{-r\tau}} \underset{\tau\to\infty}{\approx} 1-\frac{1}{2\pi}\int_{ik_i-\infty}^{ik_i+\infty} \exp[-\lambda(k)\tau]\,u(k,V)\frac{dk}{k^2-ik}\,, \tag{3.3}$$

The Ridge Property. Suppose that $\lambda(k)$ has a saddle point k_0 in the complex k-plane determined by the solution to $\lambda'(k_0)=0$. We showed in Chapter 2 that the fundamental transform is often an analytic characteristic function. As we explained in that chapter, analytic characteristic functions have the *ridge property,* which means that any saddle point must lie along the purely imaginary axis. In other words, $k_0 = iy_0$, where y_0 is a real number. This saddle point location will be confirmed in computational examples below.

The reality of the eigenvalue problem (3.2). Recall the reflection property from (**2**.2.20): $\hat{H}^*(k,V,\tau)=\hat{H}(-k^*,V,\tau)$. Combining this property with the ridge property, any saddle point must be found along $k=iy$, where $\hat{H}^*(iy,V,\tau)=\hat{H}(iy,V,\tau)$. That is: *the fundamental transform is real along the imaginary k-axis.* In turn, this shows that both the first eigenvalue and the associated eigenfunction are *real* along the imaginary axis. And finally, we can see from (3.2) that each of the coefficients of the equation will be real along that axis. In other words, to summarize: the asymptotic term structure is determined by the smallest solution to an eigenvalue problem, where the eigenvalue, eigenfunction, and associated PDE are all real-valued.[5]

An important element of the saddle point method is moving the integration contour so that it traverses the saddle point. Before we can do that, recall that (3.3) is a valid formula as long as the integration contour lies in the intersection of the fundamental strip $\alpha < \mathrm{Im}\,k < \beta$ with the strip $0 < \mathrm{Im}\,k < 1$; this is the strip of regularity. We now make the further assumption that the saddle point $k_i = \mathrm{Im}\,k = y_0$ lies within the strip of regularity[6]. If it does, then, by *Cauchy's theorem* (See Chapter 2, Appendix 1), we can move the integration contour to

---

[5] The complex-valued coefficients in (3.2) are needed for the full transform, but not for its asymptotic saddle point behavior.

[6] Practical numerical examples—see Table 6.1—show that y_0 is often close to 1/2, so this is not problematic in my experience.

$\text{Im}\, k = y_0$ without changing the value of the integral. Next, expand $\lambda(k)$ in a Taylor series about k_0:

$$\lambda(k) = \lambda(k_0 + k_r) \simeq \lambda(k_0) + \tfrac{1}{2} k_r^2 \lambda''(k_0)\,,$$

so (3.3) becomes

$$\frac{C(S,V,\tau)}{Ke^{-r\tau}} \underset{\tau\to\infty}{\approx} 1 - \frac{1}{2\pi} \exp[-\lambda(k_0)\tau] \frac{u(k_0,V)}{k_0^2 - ik_0} \int_{-\infty}^{\infty} \exp\left[-\tfrac{1}{2} k_r^2 \lambda''(k_0)\tau\right] dk_r \;.$$

Note that this last integral is over a real integration variable. We know $\lambda''(k_0) \geq 0$ because of the ridge property. Performing the integral gives us

$$\text{(3.4)} \qquad \frac{C(S,V,\tau)}{Ke^{-r\tau}} \underset{\tau\to\infty}{\approx} 1 - \frac{u(k_0,V)}{k_0^2 - ik_0} \frac{1}{\sqrt{2\pi\lambda''(k_0)\tau}} \exp[-\lambda(k_0)\tau]\,.$$

Notice that the denominator term $k_0^2 - ik_0 = y_0(1-y_0) > 0$ since, by assumption $0 < y_0 < 1$. The arbitrage bound $C(S,V,\tau) \leq Se^{-\delta\tau}$ combined with $Ke^{-r\tau} = Se^{-\delta\tau}$, implies that in (3.4) we must have $C(S,V,\tau)/Ke^{-r\tau} \leq 1$. This implies that not only is $u(k_0,V)$ real, but it's non-negative as well. That same bound also strengthens the inequality $\lambda''(k_0) \geq 0$ to $\lambda''(k_0) > 0$. Finally, comparing (3.4) with (2.3) yields a simple result for the (at-the-money) asymptotic implied volatility:

$$V_\infty^{imp}(X=0) = 8\lambda(k_0)$$

Next, we repeat the calculation for an arbitrary value for the moneyness measure *X*. In that case, (3.4) becomes:

$$\text{(3.5)} \qquad \frac{C(S,V,\tau)}{Ke^{-r\tau}} \underset{\tau\to\infty}{\approx} e^X - \frac{u(k_0,V)}{k_0^2 - ik_0} \frac{1}{\sqrt{2\pi\lambda''(k_0)\tau}} \exp[-\lambda(k_0)\tau - ik_0 X]\,.$$

But the B-S solution, for general X, has the asymptotic form:

$$\text{(3.6)} \qquad \frac{c(S,V,\tau)}{Ke^{-r\tau}} \underset{\tau\to\infty}{\approx} e^X - \sqrt{\frac{8}{\pi V\tau}} \exp\left[-\tfrac{1}{2}\left(\frac{X}{\sqrt{V\tau}} - \tfrac{1}{2}\sqrt{V\tau}\right)^2\right].$$

Comparing the two solutions (3.5) and (3.6) implies that

$$\text{(3.7)} \qquad -\tfrac{1}{2}\left(\frac{X}{\sqrt{V^{imp}\tau}} - \tfrac{1}{2}\sqrt{V^{imp}\tau}\right)^2 \underset{\tau\to\infty}{\approx} -\lambda(k_0)\tau - ik_0 X$$

After some rearrangement, (3.7) is equivalent to

(3.8)
$$\boxed{V^{imp}(X,V,\tau) \underset{\tau\to\infty}{\approx} 8\lambda(k_0) + (4-8y_0)\frac{X}{\tau} - \frac{X^2}{2\lambda(k_0)\tau^2} + O(\tau^{-3})}$$

where recall that $k_0 = iy_0$. This last equation is important because it implies that, as $\tau \to \infty$, the smile *flattens* to a common asymptotic value regardless of the moneyness *X*. And that common value is

(3.9)
$$\boxed{V_\infty^{imp} = \lim_{\tau\to\infty} V^{imp}(X,V,\tau) = 8\lambda(k_0)}$$

We will see in examples below that, when $\rho = 0$ (the symmetric case), then $y_0 = 1/2$ and the linear term in (3.8) vanishes.

4 Example I: The Square Root Model

For this model, volatility process (under risk neutrality) is $dV = (\omega - \theta V)\,dt + \xi\sqrt{V}\,dW(t)$, where the Brownian motion has correlation ρ with the stock price process. In Fig. 6.1, we showed an example of the term structure with $\omega/\theta = 0.01$ and $\xi = 0$. Next, we keep the same parameters but turn on the volatility of volatility parameter to $\xi = 1$, keeping $\rho = 0$. (We chose a value for ξ larger than would typically be measured in order to emphasize the effects).

The term structure under stochastic volatility is shown in Fig. 6.2. Now there is more structure to the plot. Instead of a monotonic evolution in τ to 10%, there is a dip to a significantly lower value when τ less than a year. At large τ, there is a clear indication of a common asymptote, just as we would expect from the theory of the last section. The new asymptotic value is no longer 10% but lower at approximately 9.92%. We found this value by applying the general theory of the previous section, as we now show.

The formulas for the fundamental transform are given at (**2**.3.1) and (**2**.3.2), taking the parameter $\gamma = 1$. (We will refer to expressions used there). We showed in Chapter 2 that the fundamental strip for this model is at least as large as the unit strip $I_0 = \{k \mid 0 < \operatorname{Im} k < 1\}$.

With k in the unit strip, then $\mathrm{Re}\, d > 0$, which leads to the limiting behaviors $f_1(t) \approx \tilde{\omega} g t$ and $f_2(t) \approx g$ as $t \to \infty$. Being careful to note the time rescaling that occurred in (**2**.3.1), this means that, as $\tau \to \infty$,

$$\hat{H}(k,V,\tau) \underset{\tau\to\infty}{\approx} \exp[-\lambda(k)\tau]\, u(k,V),$$

where

(4.1) $$\lambda(k) = -\omega g(k) = \frac{\omega}{\xi^2}\left\{[(\theta + ik\rho\xi)^2 + (k^2 - ik)\xi^2]^{1/2} - (\theta + ik\rho\xi)\right\}$$

and $$u(k,V) = \exp[g(k)V].$$

The stationary point k_0 in the complex k-plane is the solution to $d\lambda(k)/dk = 0$. This equation has two solutions:

(4.2) $$k_0 = \frac{i}{1-\rho^2}\left\{\tfrac{1}{2} - \frac{\rho}{\xi}\left(\theta \pm \tfrac{1}{2}\left[4\theta^2 + \xi^2 - 4\rho\,\theta\,\xi\right]^{1/2}\right)\right\}.$$

As promised, it's purely imaginary. As $\xi \to 0$, we want $k_0 \to i/2$ in order to reproduce the B-S solution. This limit will be correct if we choose the minus sign in (4.2). Substituting that value for k_0 into (4.1) yields

(4.3) $$\lambda(k_0) = \frac{\omega}{2(1-\rho^2)\xi^2}\left\{\left[4\theta^2 + \xi^2 - 4\rho\,\theta\,\xi\right]^{1/2} - (2\theta - \rho\xi)\right\}$$

$$= \frac{\omega}{2(1-\rho^2)\xi^2}\left\{\left[(2\theta - \rho\xi)^2 + (1-\rho^2)\xi^2\right]^{1/2} - (2\theta - \rho\xi)\right\}.$$

In the second line of (4.3), the positivity of $\lambda(k_0)$ is manifest, assuming $\omega > 0$, $\xi^2 > 0$, and $|\rho| < 1$. In fact, the limit $|\rho| \to 1$ is well-defined, and is given by

(4.4) $$\lim_{|\rho|\to 1} \lambda(k_0) = \frac{\omega}{4[2\theta - sign(\rho)\xi]}.$$

A more practical limit is $\rho = 0$. When $\rho = 0$, then (4.2) shows that the stationary point sticks at $k_0 = i/2$. This happens in general models, as you will see several times in different examples below. It's only when $\rho \neq 0$ that the stationary point moves away from $k_0 = i/2$. Which direction it moves (north or south) depends upon the sign of ρ.

Finally, the asymptotic implied volatility is given by

$$
\begin{aligned}
(4.5)\qquad V_\infty^{imp} &= \frac{4\omega}{(1-\rho^2)\xi^2}\left\{\left[4\theta^2+\xi^2-4\rho\,\theta\,\xi\right]^{1/2}-(2\theta-\rho\xi)\right\} \\
&= \frac{\omega}{\theta}+\frac{\omega\rho}{2\theta^2}\xi+\frac{\omega(-1+5\rho^2)}{16\,\theta^3}\xi^2+\frac{\omega\rho(-3+7\rho^2)}{32\theta^4}\xi^3 \\
&\qquad +\frac{\omega(1-14\rho^2+21\rho^4)}{128\theta^5}\xi^4+O(\xi^5)\,.
\end{aligned}
$$

For Fig. 6.2, the parameters are $\rho=0$, $\omega_a=0.02$, $\theta_a=2$, and $\xi_a=1$, which yields

$$
V_\infty^{imp}(\rho=0)=\frac{4\omega}{\xi^2}\left\{\left[4\theta^2+\xi^2\right]^{1/2}-2\theta\right\}=\frac{1}{25}(2\sqrt{17}-8)\,.
$$

Or, in others words $\sigma_\infty^{imp}\cong 9.92\%$.

The volatility of volatility expansion in the square root model. The second line of (4.5) shows that a volatility of volatility expansion for V_∞^{imp} exists, at least for $|\,\xi\,|$ inside a radius of convergence. Two terms of that expansion, when $\rho=0$, are $V_\infty^{imp}\cong(\omega/\theta)-\omega\xi^2/(16\theta^3)$, which yields $\sigma_\infty^{imp}\cong 9.93\%$ for the same example above. This suggests that, for models that cannot be solved exactly, the $\xi-$ expansion can provide a good approximation for σ_∞^{imp}. See Sec. 6 and 7 for an example.

The convergence of the expansion in (4.5) is determined by the power series expansion of the square root term:

$$
\left[1+\frac{(\xi^2-4\theta\rho\xi)}{4\theta^2}\right]^{1/2}.
$$

This radius is determined by considering ξ as a complex parameter. In the complex $\xi-$ plane, there are branch point singularities at $\xi=\xi^*$, where ξ^* solves $\xi^2-4\theta\rho\xi+4\theta^2=0$. If R is the distance to the solution closest to the origin; then the series will converge for $|\,\xi\,|<R$.

For example, when $\rho=0$, the branch points are at $\xi^*=\pm 2i\theta$, so the series will converge for $|\,\xi\,|<2\,|\,\theta\,|$. More generally, the branch points are found at $\xi^*=z(\rho)\theta$, where $z(\rho)$ is a solution to $z^2-4\rho\,z+4=0$. The solutions to this equation are given by $z=2\rho\pm 2i\,[1-\rho^2]^{1/2}$, which traces out a circle of radius 2 as ρ ranges from -1 to 1. Hence $|\xi| < 2|\theta|$ is the radius of convergence in the square root model for all $|\rho| \leq 1$.

In Sec. 6, we develop the ξ – expansion for V_∞^{imp} for the GARCH diffusion—in that case, we don't know if the series converges in any radius.

5 Example II: The 3/2 Model

The fundamental solution is given at (**2**.3.3). In the limit $\tau \to \infty$, we have

$$X\left(\frac{2\omega}{\xi^2 V}, \omega\tau\right) \approx \frac{2\omega}{\xi^2 V} \exp(-\omega\tau) .$$

This implies that $\hat{H}(k,V,\tau)$ again separates to the eigenfunction form:

(5.1) $$\hat{H}(k,V,\tau) \approx \exp[-\lambda(k)\tau]\; u(k,V) , \quad \text{where now}$$

(5.2) $$\lambda(k) = \omega\alpha(k)$$

$$= \frac{\omega}{\xi^2}\left\{\left[(\theta + ik\rho\xi + \tfrac{1}{2}\xi^2)^2 + (k^2 - ik)\xi^2\right]^{1/2} - (\theta + ik\rho\xi + \tfrac{1}{2}\xi^2)\right\},$$

and $$u(k,V) = \frac{\Gamma(\beta(k) - \alpha(k))}{\Gamma(\beta(k))}\left(\frac{2\omega}{\xi^2 V}\right)^{\alpha(k)} .$$

The stationary point k_0 is given by

$$k_0 = \frac{i}{1-\rho^2}\left\{\tfrac{1}{2} - \frac{\rho}{\xi}(\theta + \tfrac{1}{2}\xi^2) + \frac{\rho}{2\xi}\left[(2\theta + \xi^2)^2 + \xi^2 - 2\rho\xi\,(2\theta + \xi^2)\right]^{1/2}\right\}.$$

Again, the stationary point resides on the imaginary axis. The asymptotic implied volatility is given by

(5.3) $$V_\infty^{imp} = \frac{4\omega}{(1-\rho^2)\xi^2}\left\{\left[(2\theta + \xi^2 - \rho\xi)^2 + (1-\rho^2)\xi^2\right]^{1/2} - (2\theta + \xi^2 - \rho\xi)\right\}$$

$$= \frac{\omega}{\theta} + \frac{\omega\rho}{2\theta^2}\xi - \frac{\omega(1 + 8\theta - 5\rho^2)}{16\,\theta^3}\xi^2 - \frac{\omega\rho(3 + 16\theta - 7\rho^2)}{32\theta^4}\xi^3$$

$$+ \frac{\omega(1 - 14\rho^2 + 21\rho^4 + 32\theta^2 + 12\theta - 60\theta\rho^2)}{128\theta^5}\xi^4 + O(\xi^5) .$$

It's interesting that (5.3) may be obtained from (4.5) by making the substitution $\theta \to \theta + \xi^2/2$ in (4.5). The radius of convergence of (5.3) again vanishes with θ, but that radius has a more complicated dependence on parameters now.

6 Example III: The GARCH Diffusion Model

The GARCH diffusion model, under risk neutrality, has the volatility process $dV = (\omega - \theta V)\,dt + \xi V dW(t)$, so that the eigenvalue problem (3.2) becomes

$$(6.1) \qquad -\tfrac{1}{2}\xi^2 V^2 \frac{d^2 u}{dV^2} - \left[\omega - \theta V - ik\rho\xi V^{3/2}\right]\frac{du}{dV} + c(k)V\,u = \lambda(k)u$$

We don't have an exact solution, so we need approximate methods. In this section, we show one such method: the volatility of volatility series expansion. Previously, in Chapter 3, we showed how to use that expansion to develop the full time dependence for the fundamental transform. Now, we don't want the time dependence—only the first eigenvalue solution to (6.1). There are two unknowns: the eigenfunction $u(k,V)$ and the first eigenvalue $\lambda(k)$.

It's convenient to change variables from V to $x = c(k)V$. While this would generally make x complex-valued, the solution we need resides on the purely imaginary k-axis. That means it suffices to let k be purely imaginary and within the strip $0 < \mathrm{Im}\,k < 1$. With that restriction, $c(k)$ is a real, positive number and x is a real, positive number, just like V.

We let $u(k,V) = f(x)$, where we will suppress the explicit k-dependence. Finally, introduce the new parameters $A = c(k)\omega$, $B = \theta$, and $D = i\rho k/\sqrt{c(k)}$. All three parameters are real with k restricted as indicated. With these changes, (6.1) becomes

$$(6.2) \qquad \mathcal{L}_k f = \lambda f, \qquad (0 < \mathrm{Im}\,k < 1, \quad \mathrm{Re}\,k = 0)$$

where
$$\mathcal{L}_k f = -\tfrac{1}{2}\xi^2 x^2 \frac{d^2 f}{dx^2} - \left(A - Bx - \xi D x^{3/2}\right)\frac{df}{dx} + x\,f\,.$$

To create the series, substitute into (6.2) the formal expansions

$$\lambda = \sum \xi^j \lambda^{(j)}, \qquad f(x) = \sum \xi^j f^{(j)}(x)$$

For example, $f^{(1)}$ satisfies

(6.3) $$-(A-Bx)\frac{df^{(1)}}{dx}+\xi D\,x^{3/2}\,\frac{df^{(0)}}{dx}+x\;f^{(1)}=\lambda^{(0)}\,f^{(1)}+\lambda^{(1)}\,f^{(0)}.$$

When $\xi = 0$, we already have shown that

$$\lambda^{(0)}=c(k)\frac{\omega}{\theta}\qquad\text{and}\qquad u^{(0)}=\exp\left[-c(k)\frac{1}{\theta}\left(V-\frac{\omega}{\theta}\right)\right].$$

In terms of the new variables, this translates into

$$\lambda^{(0)}=\frac{A}{B}\;\;\text{and}\;\;f^{(0)}(x)=\exp\left[-\frac{1}{B}(x-x^*)\right],\quad\text{where}\;\;x^*=\frac{A}{B}.$$

So (6.3) can be rewritten

(6.4) $$\frac{df^{(1)}}{dx}+\frac{1}{B}\,f^{(1)}=h^{(1)}(x)\quad,$$

where $$h^{(1)}(x)=-\frac{\left(\lambda^{(1)}+\dfrac{D}{B}x^{3/2}\right)}{A-B\,x}\exp\left[-\frac{1}{B}(x-x^*)\right].$$

Now (6.4) is an ordinary differential equation with the general solution

(6.5) $$f^{(1)}(x)=Ce^{-x/B}+e^{-x/B}\int_{x_0}^{x}e^{y/B}h^{(1)}(y)dy\,,$$

where C and x_0 are constants. The solutions to an eigenvalue equation $\mathcal{L}\,f=\lambda f$ are clearly determined only up to some constant multiplier. So we need a normalization. Because $f^{(0)}(x=x^*)=1$, we will enforce the normalization $f(x=x^*)=1$. This means that $f^{(i)}(x=x^*)=0$ for all $i\geq 1$. Potentially, $f^{(1)}(x=x^*)=0$ can be achieved by choosing $C=0$ and $x_0=x^*$ in (6.5).

But (6.4) shows the integrand $h^{(1)}$ has a denominator term that vanishes at $x=x^*$, so we have to be careful. We need an assumption: suppose df/dx exists at $x=x^*$. Then, from (6.4) we see that $df^{(1)}/dx$ exists at $x=x^*$ if and only if $h^{(1)}(x=x^*)$ exists (since $f^{(1)}(x^*)=0$ by the normalization condition). By L'Hospital's rule, $h^{(1)}(x=x^*)$ exists if the numerator expression for $h^{(1)}(x)$ also vanishes at $x=x^*$. This determines $\lambda^{(1)}$; we must have

(6.6) $$\lambda^{(1)}=-\frac{D}{B}\left(\frac{A}{B}\right)^{3/2}.$$

Then we can indeed take $C = 0$, $x_0 = x*$ and satisfy the normalization. Moreover, $f^{(1)}(x)$ has now been determined:

(6.7) $$f^{(1)}(x) = e^{-x/B} \int_{x*}^{x} e^{y/B} h^{(1)}(y) dy$$

This basic argument works to all orders in the expansion. The general recursion system is, for $n = 1, 2, \ldots$

(6.8) $$\lambda^{(n)} = \left[D\, x^{3/2} \frac{d}{dx} f^{(n-1)} - \tfrac{1}{2} x^2 \frac{d^2}{dx^2} f^{(n-2)} \right] \Bigg|_{x=x*},$$

$$f^{(n)}(x) = e^{-x/B} \int_{x*}^{x} e^{y/B}\, h^{(n)}(y)\, dy\,,$$

$$h^{(n)}(x) = \frac{-1}{(A - Bx)} \left[\sum_{j=1}^{n} \lambda^{(j)} f^{(n-j)} - D x^{3/2} \frac{d}{dx} f^{(n-1)} + \tfrac{1}{2} x^2 \frac{d^2}{dx^2} f^{(n-2)} \right],$$

where terms with $(n-2)$ are omitted at $n = 1$. Applying this algorithm, we find

(6.9) $$\begin{aligned} \lambda = \frac{A}{B} - \left(\frac{A}{B}\right)^{3/2} \frac{D}{B} \xi - \frac{A^2}{2B^4}(1 - 3D^2)\xi^2 \\ + \left(\frac{A}{B}\right)^{3/2} \frac{D}{16B^4}(-3B^2 + 40A - 42AD^2)\xi^3 \\ + \frac{A^2}{32B^7}\left[4A(8 - 73D^2 + 40D^4) - B^2(8 - 27D^2)\right] \xi^4 + O(\xi^5) \end{aligned}$$

The stationary point must also be determined order by order in ξ. We find

$$k_0 = i\, \left\{ \frac{1}{2} + \left(\frac{\omega}{\theta}\right)^{1/2} \frac{\rho}{8\theta} \xi + \frac{\rho^2 \omega}{8\theta^3} \xi^2 + \left(\frac{\omega}{\theta}\right)^{1/2} \frac{\rho\left[\omega(-6 + 41\rho^2) + 6\theta^2\right]}{256\theta^4} \xi^3 + O(\xi^4) \right\}$$

As expected, k_0 is pure imaginary. The stationary point sticks at $k_0 = i/2$ if $\rho = 0$. Finally, the asymptotic implied volatility is given by

(6.10) $$\begin{aligned} V_\infty^{imp} &= 8\lambda(k_0) \\ &= \frac{\omega}{\theta} + \left(\frac{\omega}{\theta}\right)^{3/2} \frac{\rho}{2\theta} \xi + \frac{\omega^2(-1 + 7\rho^2)}{16\,\theta^4} \xi^2 + \left(\frac{\omega}{\theta}\right)^{3/2} \frac{\rho[\omega(-10 + 31\rho^2) + 6\theta^2]}{64\theta^4} \xi^3 \\ &\quad + \frac{1}{256\theta^7} [\omega^3(4 - 81\rho^2 + 157\rho^4) + 4\omega^2\theta^2(-2 + 15\rho^2)]\, \xi^4 + O(\xi^5)\,. \end{aligned}$$

A dimensionality check. Recall the time dimensions for the GARCH diffusion parameters: $[V] = 1/[t]$, $[\theta] = 1/[t]$, $[\omega] = 1/[t]^2$, $[\xi^2] = 1/[t]$. So if we write $V_\infty^{imp} = \theta\, g(\bullet)$, then $g(\bullet)$ must be a function of dimensionless ratios. With only 3 parameters with dimensions, there are only two independent ratios, so we must have

$$V_\infty^{imp} = \theta\, g\left(\frac{\omega}{\theta^2}, \frac{\xi}{\sqrt{\theta}}\right).$$

Indeed, one can check that (6.10) is equivalent to

$$\begin{aligned} g(x,z) = x &+ \tfrac{1}{2}\rho\, x^{3/2} z + \tfrac{1}{16}(-1+7\rho^2)x^2 z^2 \\ &+ \tfrac{1}{64}\rho\, [(-10+31\rho^2)x^{5/2} + 6x^{3/2}]\, z^3 \\ &+ \tfrac{1}{256}[(4-81\rho^2+157\rho^4)x^3 + (-8+60\rho^2)x^2]\, z^4 + O(z^5)\,. \end{aligned}$$

Numerical examples. We have extended (6.10) through $O(\xi^{10})$, although the expressions are too lengthy to report here. However, numerical examples showing the behavior of the partial sums through $O(\xi^{10})$ are given in Table 6.1. As one sees, the series is fairly well-behaved for typical parameter values and the partial sums tend to stabilize at higher order if θ is not too small. The series results are consistent with variational estimates, which are explained in the next section.

Table 6.1 Asymptotic Implied Volatility σ_{∞}^{imp} GARCH Diffusion Model: Series and Variational Methods

Model Parameters: $\omega_a = 0.02$, $\theta_a = 2$, $\xi_a = 1.5$.

	Correlation, ρ, between stock prices and volatility				
Series Order	**-1**	**-0.5**	**0.0**	**0.5**	**1.0**
ξ^0	10.0	10.0	10.0	10.0	10.0
ξ^2	9.8215	9.9071	9.9982	10.0946	10.1961
ξ^4	9.7870	9.8881	9.9973	10.1150	10.2418
ξ^6	9.7783	9.8828	9.9967	10.1212	10.2577
ξ^8	9.7764	9.8814	9.9964	10.1232	10.2640
ξ^{10}	9.7762	9.8811	9.9962	10.1238	10.2669
Variational	9.7759	9.8812	9.9961	10.1238	10.2708
Stationary Pt.	0.489 *i*	0.494 *i*	0.5 *i*	0.507 *i*	0.515 *i*

Notes for Tables 6.1 and 6.2 The tables show the asymptotic $(\tau \to \infty)$ implied volatility for the GARCH diffusion model: $dV = (\omega - \theta V)\,dt + \xi V dW(t)$ versus the correlation ρ. Parameters are annualized. Two methods of calculation are shown; (i) a series expansion in powers of ξ and (ii) a variational method. The series results are the partial sums. Generally, there is good agreement between the two sets of results. The agreement is better in Table 6.1 than 6.2 because the series performs better at larger θ.

Table 6.2 Asymptotic Implied Volatility σ_{∞}^{imp}
GARCH Diffusion Model: Series and Variational Methods

Model Parameters: $\omega_a = 0.01$, $\theta_a = 1$, $\xi_a = 1.5$.

	Correlation, ρ , between stock prices and volatility				
Series Order	**-1**	**-0.5**	**0.0**	**0.5**	**1.0**
ξ^0	10.0	10.0	10.0	10.0	10.0
ξ^2	9.6615	9.8161	9.9930	10.1910	10.4088
ξ^4	9.5453	9.7425	9.9851	10.2747	10.6143
ξ^6	9.5015	9.7041	9.9763	10.3271	10.7722
ξ^8	9.5001	9.6868	9.9666	10.3615	10.9163
ξ^{10}	9.5242	9.6834	9.9562	10.3833	11.0712
Variational	9.4789	9.6924	9.9577	10.3253	10.9712
Stationary Pt.	0.478 *i*	0.486 *i*	0.5 *i*	0.522 *i*	0.578 *i*

7 A Variational Principle Method

There is a deep connection between eigenvalue problems and variational principles[7]. In this section, we make that connection for our application. Very briefly, the first eigenvalue is a minimum of a certain functional. This extremal property can be exploited as a calculation tool, enabling the first eigenvalue (and hence the asymptotic implied volatility) to be estimated to high accuracy. What makes our application special is the presence of the complex-valued parameter k, a complication that requires careful handling.

We begin with the GARCH diffusion process of Sec. 6. After completing a full treatment including an example, we then extend the development to general processes.

We gave the full time-development equation for the fundamental transform at (**2**.2.19). With the volatility process given by the GARCH diffusion, we make the same change of variables as in Sec. 6, letting $x = c(k)V$, $A = c(k)\omega$, $B = \theta$, and $D = i\rho k / \sqrt{c(k)}$. In addition, we let $\hat{H}(k,V,\tau) = f(x,\tau)$, where we imply the k-dependence. Then (**2**.2.19) becomes

$$-\mathcal{L}_k f = \tfrac{1}{2}\xi^2 x^2 \frac{\partial^2 f}{\partial x^2} + \left(A - Bx - \xi D x^{3/2}\right)\frac{\partial f}{\partial x} - x f = \frac{\partial f}{\partial \tau}. \tag{7.1}$$

The *k*-plane restriction. Throughout this section, we take the parameter k to be purely imaginary and restricted to the interval $0 < \operatorname{Im} k < 1$. Because of that restriction, the new variable x is real and positive, and the coefficients in (7.1) are all real. Because of the ridge property and the martingale property, that restricted interval in the complex k-plane suffices to determine the asymptotic implied volatility for the option problem.

An auxiliary stochastic process. With our k-plane restrictions, (7.1) can be associated with the *real-valued*, auxiliary stochastic process

$$dx = \left(A - Bx - \xi D x^{3/2}\right)dt + \xi x\, dB(t), \qquad 0 < x < \infty, \tag{7.2}$$

[7] A classical and extensive reference is Courant and Hilbert (1989), Chapts IV and VI.

where $dB(t)$ is a Brownian motion. We use "auxiliary" because (7.2) is *not* where we started. We began with the GARCH diffusion under risk neutrality, which is $dV = (\omega - \theta V)\,dt + \xi V dB(t)$ —the auxiliary process has an extra term with the D coefficient.

The forward equation. Next, consider the so-called "forward equation" for the auxiliary process:

$$\frac{\partial p}{\partial \tau} = \mathcal{A}^{\dagger} p = \tfrac{1}{2}\xi^2 \frac{\partial^2}{\partial x^2}(x^2 p) - \frac{\partial}{\partial x}\left[(A - Bx - \xi D\, x^{3/2})\,p\right]. \tag{7.3}$$

Our notation is that $\mathcal{A}$ is the generator for the stochastic process (7.2) and $\mathcal{A}^{\dagger}$ is the formal adjoint. A time-independent solution to (7.3) is

$$p(x) = x^{-2-2B/\xi^2} \exp\left[-\frac{2A}{\xi^2 x} - \frac{4D\sqrt{x}}{\xi}\right] \tag{7.4}$$

We use the notation $p(x)$ to stress the positivity of the solution. When $p(x)$ can be normalized, ($\int_0^\infty p(x)dx < \infty$), it may be interpreted as the long-run stationary probability distribution for the auxiliary process[8]. But we want to emphasize that the variational theory of this section does not require that $p(x)$ be integrable. The properties that are important are (i) $\mathcal{A}^{\dagger} p(x) = 0$ and (ii) $p(x) > 0$.

The variational principle. Recall the eigenvalue problem $\mathcal{L}_k u = \lambda(k) u$ defined at (6.2), where λ is the first eigenvalue and u is the first eigenfunction. Multiply both sides by $u(x)\,p(x)$ and integrate by parts. Using $\mathcal{A}^{\dagger} p(x) = 0$ and some algebra, you can establish the formula:

$$\lambda = \frac{\int_0^\infty p(x)\left\{\tfrac{1}{2}\xi^2 x^2 [u'(x)]^2 + x[u(x)]^2\right\}dx}{\int_0^\infty p(x)[u(x)]^2\,dx} \tag{7.5}$$

if $\mathcal{a}$(i) the boundary terms from the parts integrations vanish:

$$\lim_{x\to 0,\infty} x^2 p(x) u(x) u'(x) = 0\,,$$

and $\mathcal{a}$(ii) all the integrals in (7.5) exist.

---

8 See Karlin and Taylor (1981, Chapter 15)

These are typical conditions associated with a variational method—let's call $\mathcal{A}$(i) the *endpoint conditions.* We pointed out previously that $\mathcal{L}_k u = \lambda(k)u$ is not well-defined until we specify a class of functions on which $\mathcal{L}_k$ acts. Different classes can give different eigenvalues. One natural class of functions for our problem is seen to be all twice differentiable functions $f(x)$ such that the integrals in (7.5) exist and the endpoint conditions $\mathcal{A}$(i) hold. We call such functions *admissible* and denote the set of all such function by $\mathcal{A}$, so (7.5) holds if $u \in \mathcal{A}$.

The variational principle asserts that, for all $f(x) \in \mathcal{A}$, then

$$(7.6) \qquad \lambda = \min_{f(x)\in\mathcal{A}} \left\{ \frac{\int_0^\infty p(x)\left\{\frac{1}{2}\xi^2 x^2 [\, f'(x)]^2 + x[\, f(x)]^2\right\}dx}{\int_0^\infty p(x)[\, f(x)]^2\, dx} \right\}$$

Specifically, a function $f(x)$ is admissible if

$$\mathcal{A}(\text{i}) \quad \lim_{x\to 0,\infty} x^2 p(x)\, f(x)\, f'(x) = 0\,,$$

and the integrals

$$\mathcal{A}(\text{ii}) \quad \int p(x)\, f^2 dx\,, \qquad \int p(x) x\, f^2 dx\,, \qquad \int p(x) x^2 (f')^2 dx$$

are convergent. Note that the endpoint conditions do not require that either $f(x)$ or $f'(x)$ individually exist at $x = 0,\infty$. As we stressed before, the integrability conditions do not require that $p(x)$ itself be integrable. For example, when $D < 0$, then $p(x)$ is not integrable, but $f(x) = \exp(-\alpha x)$ for $\alpha > 0$ is admissible. We use exactly this form in our computational example below.

The variational principle (7.6) follows from the *Euler-Lagrange* equations of the theory of the calculus of variations. It's a powerful tool that may be used to estimate λ to high accuracy by selecting suitable *trial* functions $f(x)$. Of course, a trial function should be admissible at the very least. In fact, for admissible $f(x)$, the inequality

$$(7.7) \qquad \lambda \le \frac{\int_0^\infty p(x)\left\{\frac{1}{2}\xi^2 x^2 [\, f'(x)]^2 + x[\, f(x)]^2\right\}dx}{\int_0^\infty p(x)[\, f(x)]^2\, dx}$$

is the tightest possible upper bound because it will be realized as an equality if $f(x)$ is chosen to be the first eigenfunction.

It's interesting that in (7.7), the only explicit parameter that appears is ξ^2. Of course, we know that the eigenvalue λ depends upon the *four* parameters of the problem: A, B, D, and ξ^2 or equivalently $\omega, \theta, \rho,$ and ξ^2. The other three parameters have not disappeared, but are contained in $p(x)$.

The case $\rho = 0$ for the GARCH diffusion. Fig. 6.2 shows an example term structure when $\rho = 0$. Note how the asymptotic implied volatility, 9.92%, is less than the deterministic value, 10%. While Fig. 6.2 is a plot of the square root model, it suggests a result for the GARCH diffusion because the two models share the same linear drift form. Indeed, the variational principle implies that, when $\rho = 0$, then σ_∞^{imp} never exceeds $(\omega/\theta)^{1/2}$ in the GARCH diffusion. Let's see why.

We assume that $\omega > 0$ and $\theta > 0$. If $\rho = 0$, then $D = 0$ and $p(x)$ is normalizable. In that case $f(x) = 1$ is admissible and (7.7) implies that

$$\lambda(k) \le \frac{\int p(x) x dx}{\int p(x) dx} = \frac{A}{B} = c(k) \frac{\omega}{\theta}.$$

The stationary point for $c(k)$ is $k_0 = i/2$, so we obtain $\lambda(k_0) \le c(i/2)\omega/\theta = \omega/(8\theta)$. In other words, when $\rho = 0$, then $V_\infty^{imp} \le \omega/\theta$. ■

When $\rho \neq 0$, then $V_\infty^{imp} > \omega/\theta$ is possible. For example, the first two terms of the $\xi -$ expansion for the GARCH diffusion at (6.10) are

$$V_\infty^{imp} = \frac{\omega}{\theta} + \left(\frac{\omega}{\theta}\right)^{3/2} \frac{\rho}{2\theta} \xi + O(\xi^2),$$

and this will be larger than ω/θ for small ξ and positive ρ. See Tables 6.1, 6.2 or Fig. 6.5 for more examples of $V_\infty^{imp} > \omega/\theta$.

Numerical example. We continue with the GARCH diffusion for a numerical example using the variational principle. Although we have suppressed the k-dependence in many formulas, to actually calculate, we need to reinstate it. More explicitly, (7.7) is a bound for $\lambda(k)$, where $k = iy$, y is real and in the interval $0 < y < 1$. The weight function is more explicitly $p(k, x)$, where

$$p(k,x) = x^{-2-2\theta/\xi^2} \exp\left\{ -\frac{\omega\,(k^2-ik)}{\xi^2 x} - \frac{4\,i\rho\,k}{\xi}\left[\frac{2x}{(k^2-ik)}\right]^{1/2} \right\}.$$

Let $\tilde{p}(y,x) = p(iy,x)$, a real positive function, given by

$$\tilde{p}(y,x) = x^{-2-2\theta/\xi^2} \exp\left\{ -\frac{\omega\,y(1-y)}{\xi^2 x} + \frac{4\rho}{\xi}\left[\frac{2xy}{(1-y)}\right]^{1/2} \right\}. \tag{7.8}$$

Then, we can calculate the asymptotic implied volatility from

$$V_\infty^{imp} \le \max_{0<y<1} \min_{f(x)\in\mathcal{A}} \left\{ \frac{8\int_0^\infty p(y,x)\left\{\frac{1}{2}\xi^2 x^2 [\,f'(x)]^2 + x[\,f(x)]^2\right\} dx}{\int_0^\infty p(y,x)[\,f(x)]^2\,dx} \right\} \tag{7.9}$$

Note that its a *maximum* over *y* because the fundamental transform has a saddle point in the *k*-plane, which happens to have a maximum in the real direction and a minimum in the imaginary direction. So the fundamental transform has a minimum as a function of *y* at the saddle point. But the eigenvalue affects the fundamental transform through a multiplicative term $\exp(-\lambda\tau)$; that means we need a maximum in the eigenvalue as a function of *y*.

Let's check the consistency of these new ideas with the series solution of Sec. 6. Choosing a suitable trial function is something of an art. Your goal is to select a function that is admissible, produces integrals that can be calculated, and captures the qualitative behavior of the first eigenfunction. For example, for the GARCH diffusion , we choose the trial function $f(x) = \exp(-\alpha x)$, where α is a parameter which is optimized. This choice for the trial function is motivated by the series solution $u(x) = \exp(-x/\theta)[1+O(\xi)]$. The integrals in (7.9) may be computed by using

$$\int_0^\infty \tau^{\mu-1} \exp\left(-s\tau - \frac{1}{\tau}\right) d\tau = 2\,s^{-\mu/2} K_\mu(2s^{1/2}), \tag{7.10}$$

where $K_\mu(\cdot)$ is the modified Bessel function of the second kind of order μ. In this example, we find that (7.9) becomes

$$(7.11)\ V_\infty^{imp} \le \max_{0<y<1} \min_{a>0} \frac{\xi^2}{g_\mu(y,a,b)}\left[g_{\mu-2}(y,a,b) + \frac{\kappa y(1-y)}{a^2} g_{\mu-1}(y,a,b)\right],$$

using $$g_\mu(y,a,b) = \left(\frac{2}{a}\right)^\mu \sum_{n=0}^\infty \left(\frac{by}{\sqrt{a}}\right)^n \frac{1}{n!} K_{\mu-n/2}(a)\,, \quad \text{and}$$

$$\kappa = \frac{32\omega}{\xi^4}, \quad b = \frac{8\rho}{\xi^2}\sqrt{\omega}\,, \text{ and } \mu = 1 + \frac{2\theta}{\xi^2}.$$

In (7.11), the minimization over the original parameter α has been replaced by a minimization over a new parameter *a*. The relationship between the two is that $a = 4\sqrt{\alpha A}/\xi$. The optimization (7.11) is very straightforward to implement in Mathematica: see Appendix 1 to this Chapter.

Numerical results from computing the right-hand-side of (7.11) are given in Tables 6.1 and 6.2. The implied volatility estimate (an upper bound) is given in the table under "Variational". And "Stationary Point" reports $k_0 = iy_0$, where y_0 is the maximizing value in (7.11). The table shows a good match to the series results, which helps support the consistency and assumptions of both approaches.

Again using the bounds from (7.11), in Fig. 6.5 we plot σ_∞^{imp} versus the correlation ρ. The other parameters are $\omega_a = 0.01$, $\theta_a = 1$, and $\xi_a = 1.5$. Since $\omega/\theta = 0.01$, the deterministic volatility value for σ_∞^{imp} is 10%. The figure illustrates the fact that σ_∞^{imp} can be higher or lower than the deterministic value, depending upon the correlation.

In Fig. 6.6 we plot σ_∞^{imp} versus the volatility of volatility ξ for $\rho = 0$ and $\rho = -0.5$. The other parameters are the same as Fig. 6.4. This figure shows that σ_∞^{imp} stays quite close to the deterministic value when $\rho = 0$, even for relatively large ξ. But, for $\rho = -0.5$, σ_∞^{imp} drops off from the deterministic value much more rapidly with ξ.

General processes. We now extend the variational principle to general risk-adjusted processes of the form $dV = \tilde{b}(V)dt + a(V)dW$, with correlation $\rho(V)$. This is the one subsection in this chapter where we assume a genuine risk-adjustment may be present. Under this general process, the evolution equation for the fundamental transform has been given at (**2**.219).

It's not useful to make exactly the same change of variable that we made for the GARCH diffusion. But we can make (**2**.2.19) similar by letting $x = V$ and $\hat{H}(k,V,\tau) = f(x,\tau)$. Then (**2**.2.19) becomes

$$\frac{\partial f}{\partial \tau} = -\mathcal{L}_k f \,, \tag{7.12}$$

where $$-\mathcal{L}_k f = \tfrac{1}{2} a^2(x) \frac{\partial^2 f}{\partial x^2} + \left[\tilde{b}(x) - ik\rho(x)a(x)x^{1/2} \right] \frac{\partial f}{\partial x} - c(k)x f \,.$$

Just as in the GARCH diffusion, we assume that $k = iy$, where y is real and in the interval $0 < y < 1$. Then, all of the coefficients in (7.12) are real-valued and we can associate it with the auxiliary process:

$$dx = \left[\tilde{b}(x) - ik\rho(x)a(x)x^{1/2} \right] dt + a(x)dB(t) \,, \quad \text{where } 0 < x < \infty \,, \; k = iy \,, \; 0 < y < 1 \,. \tag{7.13}$$

This can be written more compactly by defining the (real-valued) auxiliary drift coefficient

$$\beta_k(x) = \tilde{b}(x) - ik\rho(x)a(x)x^{1/2} \,, \tag{7.14}$$

so that (7.13) reads

$$dx = \beta_k(x)dt + a(x)dB(t) \,, \quad (0 < x < \infty \,, \; k = iy \,, \; 0 < y < 1). \tag{7.15}$$

The forward equation for the auxiliary process is

$$\frac{\partial p_k}{\partial \tau} = \mathcal{A}^\dagger p_k = \tfrac{1}{2} \frac{\partial^2}{\partial x^2} \left[a^2(x) p_k(x) \right] - \frac{\partial}{\partial x} \left[\beta_k(x) p_k(x) \right]. \tag{7.16}$$

And there is a (time-independent) solution to $\mathcal{A}^\dagger p_k = 0$ given by

$$p_k(x) = \frac{1}{a^2(x)} \exp\left[\int^x \frac{2\beta_k(y)}{a^2(y)} dy \right] \,, \tag{7.17}$$

which is the analog of (7.4). Note that $p_k(x)$ is a positive real number for all (x,k) such that $0 < x < \infty$, $k = iy$, $(0 < y < 1)$. But $p_k(x)$ is not necessarily integrable with respect to *x*.

The variational principle for the first eigenvalue then becomes

$$(7.18) \qquad \lambda(k) = \min_{f(x)\in \mathcal{A}(k)} \left\{ \frac{\int_0^\infty p_k(x)\left\{\frac{1}{2}a^2(x)[\,f'(x)]^2 + c(k)x[\,f(x)]^2\right\}dx}{\int_0^\infty p_k(x)[\,f(x)]^2\,dx} \right\}.$$

The space $\mathcal{A}(k)$ of admissible functions consists of all real-valued functions that satisfy, for $k = iy$, $(0 < y < 1)$, the conditions:

(i) $\lim_{x\to 0,\infty} a^2(x)p_k(x)f(x)f'(x) = 0$,

(ii) $\int p_k(x)[\,f(x)]^2\,dx < \infty$, $\quad \int p_k(x)x[\,f(x)]^2\,dx < \infty$,

$$\int p_k(x)a^2(x)[\,f'(x)]^2 dx < \infty .$$

Note that if a first eigenvalue exists for $k = iy$, $(0 < y < 1)$, then it must be strictly positive since every term in (7.18) is positive. So we really have a two-sided bound: $\lambda > 0$ and $\lambda <$ the upper bound of (7.18).

General process (zero correlation). Let's apply the general process variational principle to the case $\rho = 0$. In that case, the auxiliary process (7.14) is *independent of* k and coincides with the risk-adjusted volatility process. So $p_k(x)$ is independent of k. Let's assume that the risk-adjusted volatility process has a long run stationary distribution $\tilde{p}(V)$ and a finite first moment. Then $p_k(x) = \tilde{p}(V)$, $p(x)$ is integrable and $f = 1$ is admissible. If we choose $f = 1$ for a trial function, then (7.18) implies that

$$(7.19) \qquad \lambda(k) \le c(k)\frac{\int_0^\infty V\,\tilde{p}(V)\,dV}{\int_0^\infty \tilde{p}(V)dV},$$

The stationary point for the right-hand-side of (7.19) is, as we expect, at $k_0 = i/2$, where $c(i/2) = 1/8$. Moreover, since $\tilde{p}(V)$ is integrable, let's normalize the denominator to 1. Then, we have the bound:

$$(7.20) \qquad V_\infty^{imp} \le \int_0^\infty V\,\tilde{p}(V)\,dV\,. \qquad (\rho = 0) \qquad \blacksquare$$

Let's check this result for the exactly solvable models. For example, for the 3/2 model, it's easy to find the stationary distribution

$$\tilde{p}(V) = CV^{-3-2\theta/\xi^2}\exp\left[-2\omega/(V\xi^2)\right],$$

where C is the normalization constant. For simplicity, assume $\omega, \theta > 0$. Then, (7.20) reads

$$V_\infty^{imp} \le \frac{2\theta}{2\theta + \xi^2} \frac{\omega}{\theta} \,. \quad \text{(3/2 model)}$$

This can be proven correct using the exact solution (5.3). It's a tighter bound than simply the deterministic limit ($\xi^2 = 0$).

A second check is any model with a linear drift: $dV = (\omega - \theta V)\, dt + a(V)\, dW(t)$. In the case of linear drift models, we proved in Appendix 5.1 (Example 1) that the long-run expected volatility is always ω / θ, regardless of $a(V)$. So for all linear drift models, (7.20) reads $V_\infty^{imp} \le \omega / \theta$, which was our previous result under the GARCH diffusion alone.

Finally, we could relax the assumption that $\tilde{p}(V)$ have a first moment, since the inequality (7.20) also makes sense if the right-hand-side is $+\infty$.

An open issue. Suppose you've solved the PDE problem (**2**.2.19) for the fundamental transform $\hat{H}(k,V,\tau)$. Your solution turns out to be a regular function in the complex k-plane in the strip $\alpha < \mathrm{Im}\, k < \beta$. Next, you let $k = iy$, where $\max[0,\alpha] < y < \min[1,\beta]$. As $\tau \to \infty$, you find that $\hat{H}(k,V,\tau) \approx \exp[-\tilde{\lambda}(k)\tau]\ \varphi(k,V)$.

Separately, with k in the same interval, you've found $\lambda(k)$, the first eigenvalue solution to $\mathcal{L}_k u = \lambda(k) u$, $u \in \mathcal{A}(k)$, where $\mathcal{A}(k)$ is the class of admissible functions defined in this section.

The open issue: is it always true that $\lambda(k) = \tilde{\lambda}(k)$? In other words, we've really just summarized the developments in Secs. 3 and 6, and are asking if they always lead to the same value for the asymptotic implied volatility. If they don't, then the conditions that define the function space $\mathcal{A}(k)$ must be revised.

8 A Differential Equation (DSolve) Method

In this section, we explain how to find the asymptotic implied volatility by solving a differential equation[9]. Numerically, we do this with Mathematica's **`DSolve`** function (actually **`NDSolve`**, to be precise)—hence the reference in the section title.

The method is very fast and produces values in just a couple seconds of desktop computer time. The variational method can be fast, too, with only a single parameter being optimized. But if you want higher accuracy in the variational method, you have to develop more complex trial functions, with more parameters. As we indicated, this is something of an art. In contrast, the method in this section, if you can set it up, can be made arbitrarily accurate just by adjusting function arguments.

A tradeoff is that the method in this section requires a certain asymptotic analysis, which is explained below. The method works for the GARCH diffusion, which is one of our main interests, because we can perform that analysis. For other models, you have to investigate.

Consider again the eigenvalue problem under GARCH diffusion process, given at (6.1) and we repeat here for convenience

$$(8.1) \qquad -\tfrac{1}{2}\xi^2 V^2 \frac{d^2u}{dV^2} - \left[\omega - \theta V - ik\rho\xi V^{3/2}\right]\frac{du}{dV} + c(k)V\,u = \lambda(k)u\,.$$

As before, consider k a purely imaginary parameter: $k = iy$ and y is in the interval $0 < y < 1$. So all of the coefficients in (8.1) are real numbers.

It makes the discussion simpler if we do a rescaling first, so multiply both sides of (8.1) by $2/\xi^2$, and define new (real) parameters

$$\tilde{\omega} = \frac{2}{\xi^2}\omega\,, \quad \tilde{\theta} = \frac{2}{\xi^2}\theta\,, \quad \tilde{d} = \frac{2ik\rho}{\xi}\,, \quad \tilde{c} = \frac{2}{\xi^2}c\,, \quad z = \frac{2}{\xi^2}\lambda\,.$$

Then (8.1) becomes

$$(8.2) \qquad V^2u'' + \left(\tilde{\omega} - \tilde{\theta}V - \tilde{d}V^{3/2}\right)u' - \tilde{c}V\,u + z\,u = 0\,.$$

---

[9] The method in this section is adapted from a similar procedure in Aslanyan and Davies (1998)

We can find the first eigenvalue by the following procedure. First, forget that z in (8.2) is related to an eigenvalue and just think of it a parameter that is fixed at some real value, say 6. Then, it's possible to develop asymptotic solutions for (8.2) both as $V \to 0$ and $V \to \infty$, which are singular points. Because (8.2) is a second order equation, there are two such solutions in any regime. But the one we report is the smaller one. Exactly how to do this is explained in Chapter 10; here we merely quote the results:

First, as $V \to 0$, we find that the "well-behaved" solution has the form:

(8.3) $$u \approx a_0\left[1 - \frac{z}{\tilde{\omega}} V\right] + O(V^{3/2}),$$

where a_0 is arbitrary. At the other extreme, as $V \to \infty$, we find that the well-behaved solution has the form:

(8.4) $$u \approx \exp\left[\left(\beta - \tilde{d}\right)\sqrt{V}\,\right] V^{\left(\frac{1}{4} - \frac{\alpha}{2} + \frac{\tilde{\theta}}{2}\right)}\left[b_0 + \frac{b_1}{\sqrt{V}} + O\left(\frac{1}{V}\right)\right],$$

where $\alpha = \dfrac{\tilde{d}(1 + 2\tilde{\theta})}{2\beta}$ and $\beta = -\dfrac{2}{\xi}\eta(k) = -\dfrac{2}{\xi}\sqrt{k^2(1-\rho^2) - ik}$

and b_0 and b_1 are constants that play no role. In general, the method of this section "works" whenever you can develop asymptotic solutions to the eigenvalue equation. This will be true in many models of interest. Next, consider the function

(8.5) $$g(V) = \frac{u'(V)}{u(V)}.$$

This function satisfies the *first order* (non-linear) differential equation, called the *Riccati equation*:

(8.6) $$V^2 \frac{dg}{dV} + V^2 g^2 + \left(\tilde{\omega} - \tilde{\theta} V - \tilde{d} V^{3/2}\right) g - \tilde{c} V + z = 0$$

Now pick a small value $V_{\min}$, a large value $V_{\max}$ and an arbitrary point a in between: $V_{\min} < a < V_{\max}$.

We can solve (8.6) in the interval $V_{\min} \le V \le a$ by starting the solution at $V_{\min}$. We start the solution by using (8.3), which implies that for small enough $V_{\min}$,

(8.7) $$g(V_{\min}) \approx -\frac{z}{\tilde{\omega}}.$$

Call this solution $g_0(V,z)$. Similarly, we can solve (8.6) in the interval $a \le V \le V_{\max}$ by using (8.4), which implies that for large enough $V_{\max}$.

$$g(V_{\max}) \approx \frac{(\beta - \tilde{d})}{2\sqrt{V_{\max}}} + \frac{(1 - 2\alpha + 2\tilde{\theta})}{4V_{\max}}. \tag{8.8}$$

Call this solution $g_1(V,z)$. Finally, define the function

$$F_a(z) = g_1(a,z) - g_0(a,z) = \frac{u_1'(a,z)u_0(a,z) - u_0'(a,z)u_1(a,z)}{u_0(a,z)u_1(a,z)}. \tag{8.9}$$

Now for a general value of *z*, the solution which behaves like (8.3) as $V \to 0$, if continued beyond the point $V = a$, will *not* behave like (8.4) as $V \to \infty$. There's a second solution that grows much more rapidly than (8.4) as $V \to \infty$; call that one the "ill-behaved" solution (see Chapter 10 for its form). For an arbitrarily chosen value of *z*, if you start the solution with (8.3), and continue that solution beyond the point $V = a$, you'll get a mixture of the well-behaved solution and the ill-behaved solution as $V \to \infty$.

But, for $z = z_0 \equiv 2\lambda/\xi^2$, where λ is the first eigenvalue, the solution $u_0(V,z_0)$, if it was continued beyond $V = a$, would be found proportional to the well-behaved solution $u_1(V,z_0)$, at least in the limit where $V_{\min} \to 0$ and $V_{\max} \to +\infty$. If $u_0(V,z_0) = m\,u_1(V,z_0)$, with *m* a constant, then the numerator in (8.9) vanishes and the denominator is proportional to $u^2(a,z_0)$, the square of the first eigenfunction.

If you increase *z* from zero, the first value at which $F_a(z)$ vanishes must then be the first (smallest) eigenvalue. Moreover, since we know the first eigenfunction $u(a,z_0)$ is positive for all *V*, the denominator in (8.9) will not vanish when the numerator does. To summarize, in the limit where $V_{\min} \to 0$ and $V_{\max} \to +\infty$, the first eigenvalue $\lambda = \xi^2 z_0/2$, where z_0 is the first (smallest) zero of $F_a(z)$ on the real positive *z*-axis.

In Mathematica, the **`NDSolve`** function easily finds numerical solutions to (8.6), creating $F_a(z)$. Then, **`FindRoot`** finds the zero z_0 of $F_a(z)$. All this happens when the parameter *k* is fixed at a pure imaginary value in the vicinity of $k = i/2$. That is $z_0 = (2/\xi^2)\lambda(k)$ and finally we use **`FindMinimum`** to find the stationary value k_0. The code is in the Appendix to this chapter.

A by-product of the calculation of λ is that you then have available the full function $g(V, z_0)$, which is defined over the entire range $V_{\min} \le V \le V_{\max}$ by

$$g(V, z_0) = \begin{cases} g_0(V, z_0) & V_{\min} \le V \le a \\ g_1(V, z_0) & a \le V \le V_{\max} \end{cases}$$

Note that $g(V, z_0)$ is continuous at $V = a$ for any values of $V_{\min}$ and $V_{\max}$ because $g_0(a, z_0) = g_1(a, z_0)$. Then, the first eigenfunction is given by the limiting value, as the boundaries become exact, of

$$u(V) = \exp\left[\int_a^V g(x, z_0)\, dx\right] \tag{8.10}$$

In Mathematica, the expression (8.10) evaluates extremely rapidly because $g(x, z_0)$, being the result of a solution to a differential equation is an "interpolating function" and such functions are rapidly integrated. We used (8.10) to produce the plots shown in Fig. 6.4. This code is also given in the Appendix.

The eigenvalues are independent of a in the limit that $V_{\min} \to 0$ and $V_{\max} \to \infty$. In practice, there's a very weak dependence with finite endpoints. Since a is a volatility value, a natural choice for the GARCH diffusion and the one we selected was $a = \omega / \theta$. A brief sensitivity analysis showed very little difference in results if the value was 50% higher or lower.

Numerical results are shown in Table 6.3 below. As you can see, the values for the asymptotic implied volatility are virtually indistinguishable from the variational method results. The method is very straightforward, fast, and should be easy to adapt to many models.

Fig. 6.5 Asymptotic Implied Volatility vs Correlation: GARCH Diffusion Model

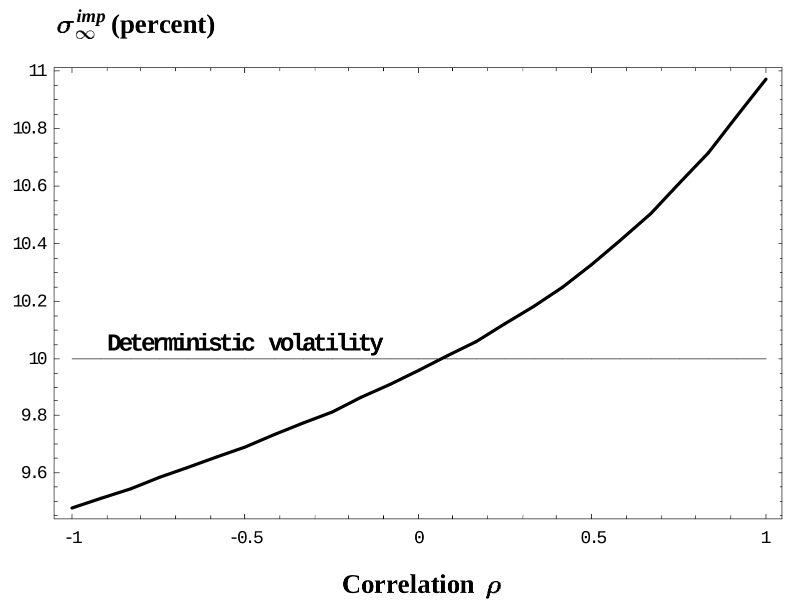

Notes. The figure shows the asymptotic implied volatility for the GARCH diffusion model $dV = (\omega - \theta V)\,dt + \xi V dW(t)$ versus the correlation parameter ρ. The other parameters are $\omega_a = 0.01$, $\theta_a = 1$, and $\xi_a = 1.5$. Since $\omega / \theta = 0.01$, the deterministic volatility value for σ_{∞}^{imp} is 10%. The figure illustrates the fact that σ_{∞}^{imp} can be higher or lower than the deterministic value, depending upon the correlation. The values are upper bounds calculated from a variational method, but both a series and a differential equation method produce the same plot.

Fig. 6.6 Asymptotic Implied Volatility vs. Volatility of Volatility: GARCH Diffusion Model

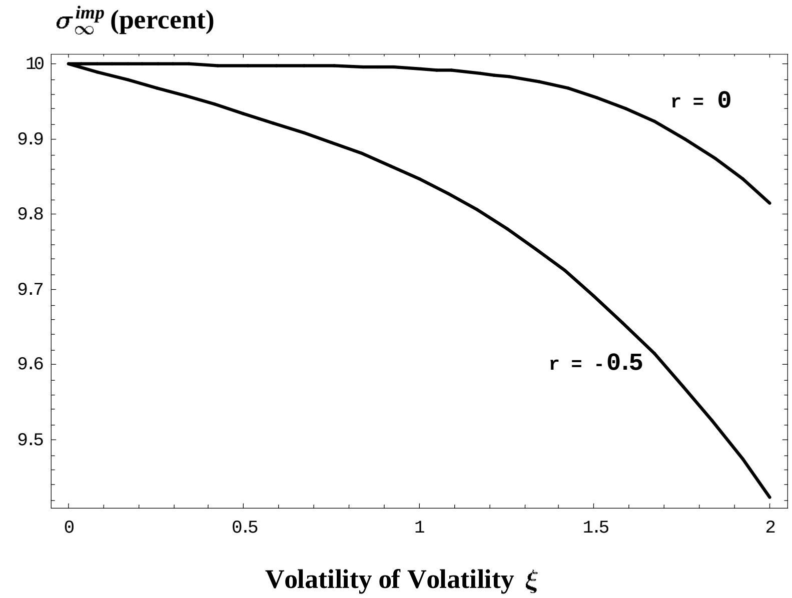

Notes. The figure shows the asymptotic implied volatility for the GARCH diffusion model $dV = (\omega - \theta V)\,dt + \xi V dW(t)$ versus the volatility of volatility parameter ξ. The other parameters are $\omega_a = 0.01$, $\theta_a = 1$. This figure shows that σ_{∞}^{imp} stays quite close to the deterministic value (10%) when $\rho = 0$, even for relatively large ξ. But, for $\rho = -0.5$, σ_{∞}^{imp} drops off from the deterministic value much more rapidly with ξ. The values are upper bounds calculated from a variational method.

Table 6.3 Asymptotic Implied Volatility σ_{∞}^{imp} (GARCH Diffusion) Variational and Differential Equation (DSolve) Methods

I. Model Parameters: $\omega_a = 0.02$, $\theta_a = 2$, $\xi_a = 1.5$.

	Correlation, ρ, between stock prices and volatility				
Method	**-1**	**-0.5**	**0.0**	**0.5**	**1.0**
(i) Variational					
σ_{∞}^{imp}	9.7759	9.8812	9.9961	10.1238	10.2708
Stationary Point	0.489 *i*	0.494 *i*	0.5 *i*	0.507 *i*	0.515 *i*
(ii) DSolve					
σ_{∞}^{imp}	9.7759	9.8812	9.9961	10.1237	10.2701
Stationary Point	0.490 *i*	0.494 *i*	0.499 *i*	0.507 *i*	0.517 *i*

II. Model Parameters: $\omega_a = 0.01$, $\theta_a = 1$, $\xi_a = 1.5$.

	Correlation, ρ, between stock prices and volatility				
Method	**-1**	**-0.5**	**0.0**	**0.5**	**1.0**
(i) Variational					
σ_{∞}^{imp}	9.4789	9.6924	9.9577	10.3253	10.9712
Stationary Point	0.478 *i*	0.486 *i*	0.5 *i*	0.522 *i*	0.578 *i*
(ii) DSolve					
σ_{∞}^{imp}	9.4785	9.6919	9.9570	10.3243	10.9649
Stationary Point	0.478 *i*	0.488 *i*	0.5 *i*	0.521 *i*	0.577 *i*

Notes. The panels show the asymptotic $(\tau \to \infty)$ implied volatility for the GARCH diffusion model: $dV = (\omega - \theta V)\,dt + \xi V dW(t)$ versus the correlation ρ . Parameters are annualized. Two methods of calculation are shown: (i) a variational method and (ii) a differential equation method (DSolve). The results are extremely close. While both methods produce values in just a couple of seconds in Mathematica, the DSolve method ran the fastest and can be made arbitrarily accurate.